TALLINN UNIVERSITY OF TECHNOLOGY
School of Information Technologies

Kristjan Kõuts 204769IVEM

# Development of a User Programmable Battery Management System for an Electric Scooter

Master's thesis

Supervisor: Kaiser Pärnamets
Master’s degree

Tallinn 2022

TALLINNA TEHNIKAÜLIKOOL
Infotehnoloogia teaduskond

Kristjan Kõuts 204769IVEM

# Seadistatava akuhaldussüsteemi arendamine elektrilisele tõukerattale

Magistritöö

Juhendaja: Kaiser Pärnamets
Magistrikraad

Tallinn 2022

# Author’s declaration of originality

I hereby certify that I am the sole author of this thesis. All the used materials, references to the literature and the work of others have been referred to. This thesis has not been presented for examination anywhere else.

Author: Kristjan Kõuts

09.05.2022

# Abstract

In this thesis, a battery management system is developed for an electric scooter. The battery management system is needed to keep the battery pack in safe operating area in terms of voltage, current and temperature and to prolong its lifespan. The battery management system is user programmable which means that the safety limits can be configured according to the needs of the user. The battery management system requirements are set according to the concept of the scooter itself and the market research of similar products. The hardware design, including schematics and layout, is based on the requirements. Firmware is also self-developed and the work principles are described. The system is tested, the conclusions are drawn and the suggestions for future work are given in the summary.

This thesis is written in English and is 34 pages long, including 6 chapters, 23 figures and 4 tables.

# Annotatsioon

Seadistatava akuhaldussüsteemi arendamine elektrilisele tõukerattale

Antud lõputöös arendatakse akuhaldussüsteemi elektrilisele tõukerattale. Akuhaldussüsteemi on vaja, et hoida akupakki lubatud pinge, voolu ja temperatuuri piirides ning akupaki eluea pikendamiseks. Akuhaldussüsteem disainitakse kasutaja poolt programmeeritavaks, et eelmainitud piire muuta vastavalt vajadusele. Akuhaldussüsteemi nõuded on määratud johtuvalt tõukeratta kontseptsioonist ja teistest sarnastest akuhaldussüsteemidest, mis saadaval on. Riistvara disain, nii skeemi kui trükkplaadi oma, põhineb seatud süsteemi nõuetel. Lõputöös käsitletakse ka tarkvara disaini ning selgitatakse selle töö põhimõtteid. Töö kokkuvõttes tehakse järeldused süsteemi testimisest ning antakse soovitused edasiseks tööks.

Lõputöö on kirjutatud inglise keeles ning sisaldab teksti 34 leheküljel, 6 peatükki, 23 joonist, 4 tabelit.

# List of abbreviations and terms

| | |
|---|---|
| ADC | Analog-to-digital converter |
| BMS | Battery management system |
| CAN | Controller area network |
| CPU | Central processing unit |
| DC | Direct current |
| ESD | Electrostatic discharge |
| GPIO | General purpose input/ output |
| $I^2C$ | Inter-integrated circuit |
| IC | Integrated circuit |
| LiFePO4 | Lithium iron phosphate |
| Li-ion | Lithium-ion |
| LQFP | Low-profile quad flat package |
| MCU | Microcontroller |
| MOSFET | Metal–oxide–semiconductor field-effect transistor |
| PCB | Printed circuit board |
| $R_{thJA}$ | Maximum junction-to-ambient thermal resistance |
| RTOS | Real time operating system |
| SMD | Surface mount device |
| SoC | State of charge |
| SoH | State of health |
| SWD | Serial wire debug |
| TVS | Transient-voltage-suppression |
| UML | Unified modeling language |
| USB | Universal serial bus |

# Table of contents

# List of figures

# List of tables

# 1 Introduction

This thesis is based on a personal project of building a custom electric scooter. However, the focus of current thesis is only on the development of a battery management system (BMS). The electric scooter is built for personal urban transportation and to use the theoretical knowledge and skills gained from the university.

Apart from the basic functionalities of an electric scooter, the electric vehicle will have a regenerative braking which is also one of the requirements for the battery management system. In addition, the scooter will have a display for estimated driving range that affects the design of the BMS with a need for a communication protocol.

As the development of the custom electric scooter is on going, the battery management system is designed to be user programmable to adapt to the changes of the system that might come such as changing the motor or the motor inverter or tuning the dynamic characteristics of the scooter like acceleration for example.

## 1.1 State of the art overview

As the number of electric vehicles on the roads is increasing, there is also an increasing need to monitor, manage, and maintain batteries of these electric vehicles. There are many different vehicles starting from electric scooters and ending up with electric cars. They also have different battery packs with different cells, configurations, voltages, energies etc. One thing those different packs have in common is the need for a battery management system. This is important to prolong the battery's lifetime and to avoid failures.

A battery management system monitors and manages the main parameters of the battery pack – voltage, current and temperature. More advance systems may monitor more complex parameters such as state of charge (SoC) and state of health (SoH) of the battery pack for example. There is no complete list of parameters a BMS must monitor as the requirements and system complexity depends on the application. However, accurate monitoring of current, voltage and temperature is critical, as overcharging a battery can

cause a thermal runaway or even an explosion [1, 2]. In addition, over discharging may render a battery useless. Each battery cell or cells in parallel are monitored separately to avoid cell failures.

Usually in electric vehicle battery packs the cells are connected in series to increase the voltage and in parallel to increase the capacity of the system. A failure of a single cell could lead to a failure of the whole battery pack. Therefore it is important to have a reliable battery management system to avoid failures and to keep the battery pack and the user safe. In addition, the quality of the battery management system directly impacts distance vehicle can travel with one charge and maximizes the batteries overall lifetime.

### 1.1.1 Battery chemistry

Lithium-ion (Li-ion) batteries are most commonly used in EVs due to their high specific energy compared to other battery chemistries such as lead-acid, nickel-metal hydride, nickel-cadium etc (Figure 1). High specific energy is important in transportation to achieve greater battery capacities while reducing the mass of the vehicle as battery packs tend to be one of the heaviest parts.

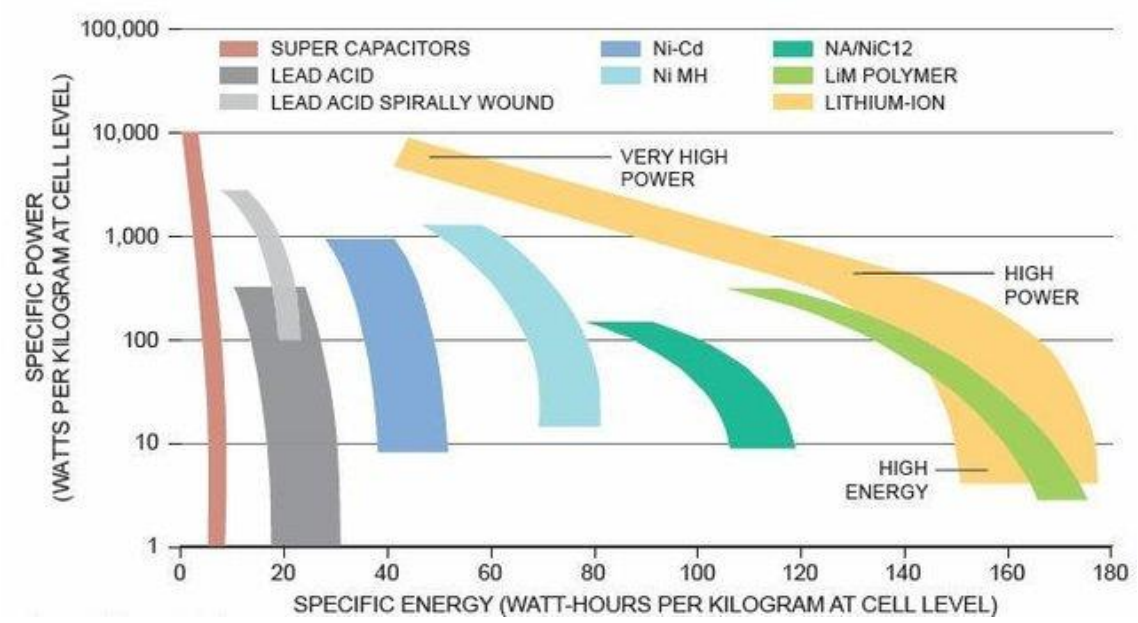


Figure 1. Different battery chemistries specific energy vs specific power [5].

The evolution of specific energy of rechargeable batteries over the past 130 years has been remarkable (Figure 2). The evolution has been rather quick since 1990s when many mobile technologies such as cell phones, laptops, music players, video games etc got

popular. Back then the first commercial Li-ion battery had the specific energy around 90 Wh/kg. The specific energy was doubled to about 180 Wh/kg in late 2008/2009. Investments in electrifying the vehicles, energy storage, clean energy etc accelerated the development of Li-ion batteries. Nowadays the specific energy of commercially available cells can reach approximately 280 Wh/kg.

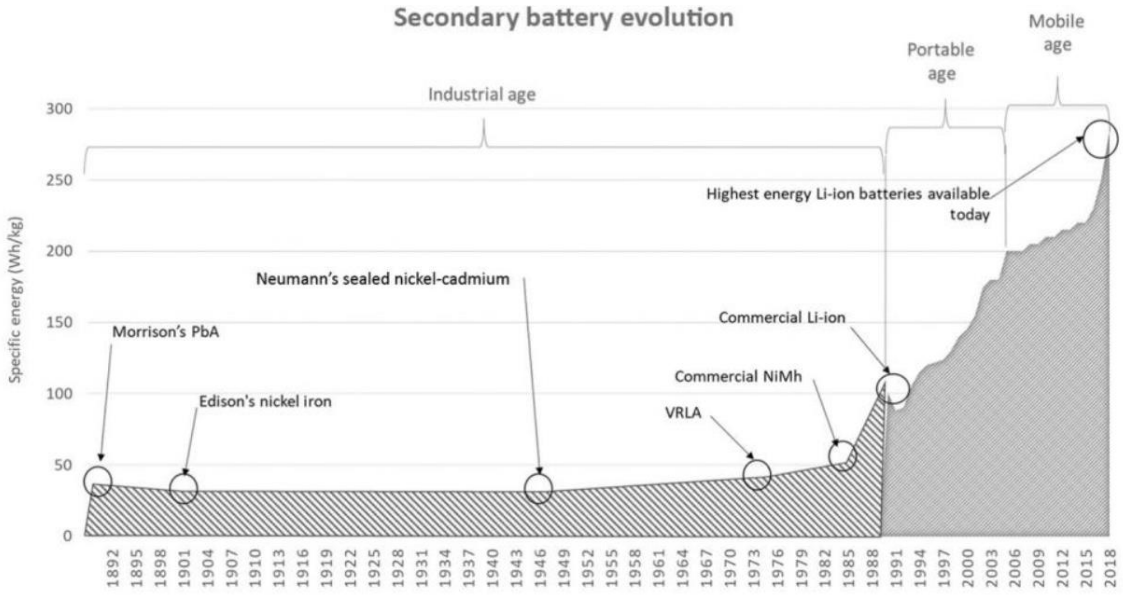


Figure 2. Modern battery specific energy over time [4].

### 1.1.2 Topologies

In vehicle BMS systems there are three common topologies used: centralized, semi-distributed/modular and distributed. In centralized BMS system all the electronics are on one printed circuit board (PCB). This includes for example the measurement circuit, the microcontroller (MCU) with communication lines, output control, the balancing schematics etc. The advantage of centralized BMS is compact structure, high reliability and low cost. It is generally used for light EVs such as electric scooters, bicycles etc.

In modular or semi-distributed architecture one of the most common topology is master-slave topology which means there are several slave PCBs monitoring a number of battery cells and they all communicate with master PCB. The master will control the battery pack output and status. Slaves usually only send the measurement data to master and have balancing circuits on them. Semi-distributed topology is found in medium sized battery packs with medium voltage and capacitance.

In distributed topology there is a PCB on every battery cell or module that measures the voltage and has balancing circuit on it. The measurement PCBs communicate with one master PCB that monitors the whole pack state. This topology is used mainly for electric cars.

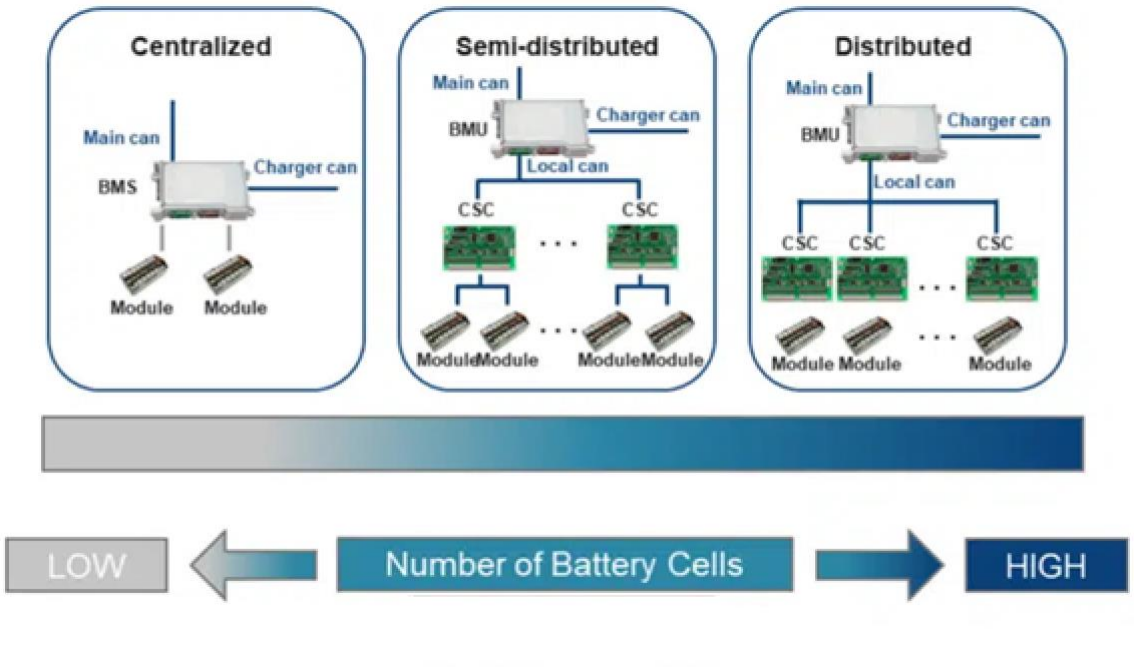


Figure 3. Different BMS topologies [6].

### 1.1.3 Products on the market

There is a variety of products available on the market with different topologies, number of measurable cells, for different battery chemistries etc. Three different products have been compared in this thesis. Two of them, DieBieMs [4] and Ennoid [5] are open-source projects and Daly DL15S [6] is from a web store.

DieBieMS is designed for electric vehicles such as electric scooters and skateboards. However, this product has separate ports for charging and discharging. This eliminates the possibility to use regenerative braking. As regenerative braking is one of the system requirements it is therefore excluded.

Ennoid battery management system uses modular architecture and master-slave topology. The electric scooter battery pack, for what this thesis battery management system design is aimed to, has only one module and therefore this topology is not the reasonable. In

addition, Ennoid BMS needs an external contactor to switch the output of the battery pack which takes extra space in the battery compartment on the scooter or in the battery pack.

Daly DL15S  is a non-configurable BMS that comes with predefined voltage, temperature and current limits. This product is designed for a particular cell chemistry (LiFePO4) and cannot be used with other types that have different voltage protection limits set by cell manufacturer. In addition, it does not have any communication protocol nor a proper documentation.

**Table 1. Examples of products available on the market.**

| | DieBieMs [7] | Ennoid [8] | Daly DL15S [9] |
|---|---|---|---|
| User programmable | Yes | Yes | No |
| Topology | Centralized | Modular | Centralized |
| Regenerative braking capability | No | Yes | No |
| Max power [W] | ~3500 | ~2500 | ~3000 |
| Need for an external contactor | No | Yes | No |
| Documentation (open source) | Yes | Yes | No |
| Communication | USB, CAN | USB, UART, $I^2C$, CAN | N/A |

## 1.2 Problem statement

Most of the products on the electric scooter and electric bike battery management system market are not user programmable. The existing solutions offer predefined limits for overvoltage, undervoltage, overcurrent, under temperature and over temperature protection that cannot be changed. Due to different battery pack configurations, applications and specific cell parameters the limits of previous parameters need to be configurable. In addition, there are important aspects usually unknown for available products such as sampling rates, accuracy, schematics, bill of materials, proper technical documentation etc.

On the other hand, majority of open-source projects have adequate technical documentation but have separate connectors for charging and discharging which eliminates the possibility to use regenerative braking on the scooter. To add, some projects have unreasonable topology for electric scooter application.

## 1.3 Thesis task specification

The aim of this thesis is to design a user programmable battery management system hardware and software that protects the battery with user set and programmed voltage, current and temperature limits. Schematics, printed circuit board layout and software will be designed and the prototype will be assembled, followed by software development. System properties will be verified by real life measurements.

# 2 System requirements

Most of the system requirements are directly related to keeping the battery cells and battery pack in safe limits. Some requirements are based on the whole scooter and it's other components design. For example, the number of cells and therefore the voltage is one of the standards in electric micro mobility vehicle battery packs and motor controllers.

The BMS must be able to measure each single Li-ion cell (or cells in parallel) voltage range which is 3.0-4.2 V as Li-ion is the most suitable battery chemistry for electric scooter due to its specific energy. The maximum voltage it should be able to measure is at least 50,4 V. That voltage is equal to 12 fully charged Li-ion battery cells connected in series with a maximum single cell voltage of 4,2 V. 12 cells in series is one of the standards in micromobility battery packs. It will be a bonus if the BMS could measure other battery chemistry voltage ranges as well.

The battery must be protected against overcurrent, overdischarge, overcharge, overtemperature and undertemperature while charging and discharging. The maximum limits are set with the datasheet of the battery cells [10] and the battery pack configuration. To prolong the battery pack's lifespan, cell balancing circuit must be implemented. As the battery cells have always some tolerances and they are never identical in terms of their parameters, they tend to age and lose capacity differently. At some point during their usage the SoC of different cells will differ from each other. Two methods are used to solve the problem. Either passive or active balancing. The first one is simpler, but also has higher power losses. The principle of passive balancing is to discharge the cells with higher SoC to the SoC of the least charged cell. On the other hand, active balancing charges the cells with lower SoC with the energy from higher SoC cells.

There are three non-functional requirements that the author has set that are not directly related to protecting the battery pack. Firstly, one power connector for battery pack that is used for charging and discharging the battery, which also enables the battery to be used

for regenerative braking. This is needed so extend the scooters driving range as regenerative braking charges the battery. Secondly, controller area network (CAN bus) communication protocol for sending BMS data to motor controller for power limiting with low SoC and to decrease the charging currents with low temperatures for example. As the inverter has CAN bus for external communication, the BMS communication protocol was chosen based on that.

Third requirement is that the PCB must have connectors and output switching circuit for heating elements. That is needed to heat up the battery pack during cold weathers to use regenerative braking. The temperature impacts the battery pack performance significantly as it affects the internal resistance and therefore its capacity because with higher internal resistance cell power losses are higher. Li-ion battery cells chemical-reaction activity and charge-transfer velocity decreases with cold temperatures which reduces the energy and power capabilities and may cause performance failures [11].

**Table 2. System requirements.**

| | |
|---|---|
| Number of cells measured | 12 |
| Maximum voltage | > 50,4 V |
| Maximum power | > 1250 W |
| Number of temperature measurements | >= 2 |
| Short circuit/overcurrent protection | > 35 A |
| Overdischarge protection per cell | 3,0 ± 0,05 V |
| Overcharge protection per cell | 4,2 ± 0,05 V |
| Overtemperature protection | > 50 °C |
| Undertemperature protection | < -5 °C |
| Precharge | Yes |
| Cell balancing | Yes |
| Regenerative braking | Yes |
| Battery pack heating | Yes |
| Communication protocol | CAN |

# 3 Hardware design

## 3.1 Introduction

The design process is based on V-model [3]. The high-level design starts with market research to get to know the state-of-the-art. After being familiar with similar products and their possible pros and cons, it is time to plan the concept and write down the system requirements. After that schematics and PCB layout design can start. Low-level design ends with software design.

The order for testing is vice-versa compared to designing. When designing started with high-level design and ended with low-level, it is the opposite for testing. Testing phase starts with software testing, followed by schematics testing, system testing and finally the whole product testing. After each testing level there is a review of the design and redesign, if necessary. The process is illustrated in the following figure (Figure 4).

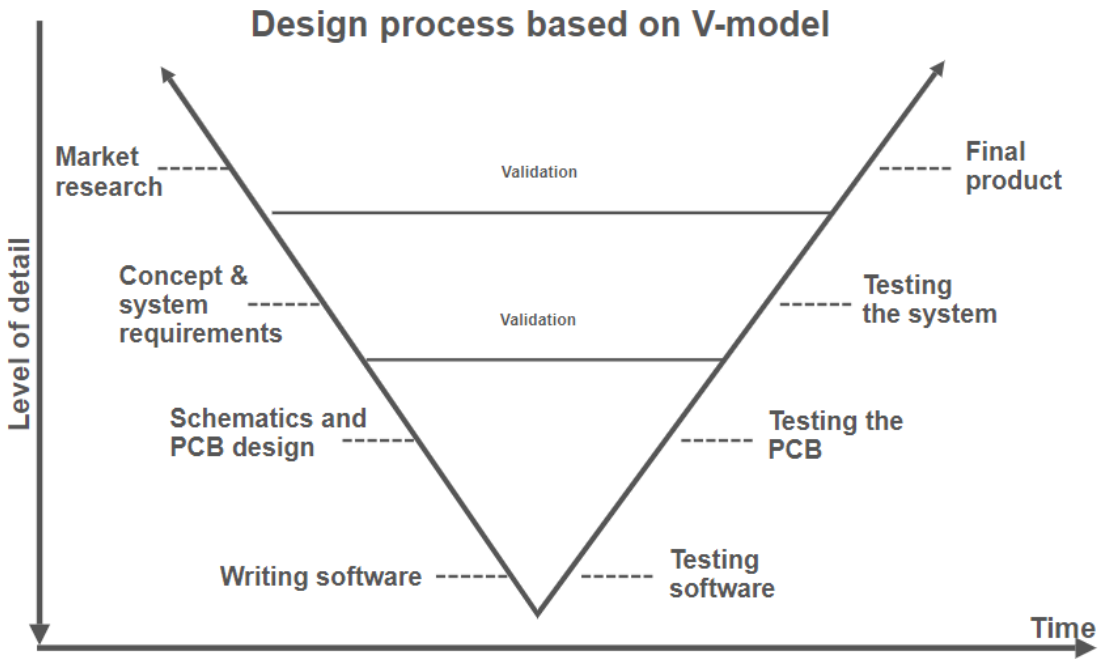


Figure 4. Design process based on V-model. [3]

The high-level system architecture is displayed in the following figure (Figure 5) is based on the system requirements and it is the input for schematics design. The BMS must monitor battery pack and cell voltages, pack current and temperature.

With this information it can protect the battery from various hazards such as overdischarging, short circuit or charging with low temperatues for example. Scooter identification will be performed to avoid switching the output falsely, leaving the battery with voltage on it's connector pins. The fault criteria and the error limits can be set with programming so the same BMS could be used in different applications or with different cells or with different battery pack configuration and limits.

Precharge is needed to avoid high inrush currents on capacitive loads when switching on the output of the battery pack. For example in electric scooter the motor controller has a DC link capacitors on 48 V line. Unlimited current could stress or damage the controller and the BMS. Output can be switched on after a successful precharge to start riding with the scooter and must be switched off after getting into error state. Cell balancing was briefly explained in the previously.

Available energy and SoC estimations are needed to integrate driving range estimation to avoid leaving the driver on the road with an empty battery pack. Communication protocol is needed to send the data to motor controller and display.

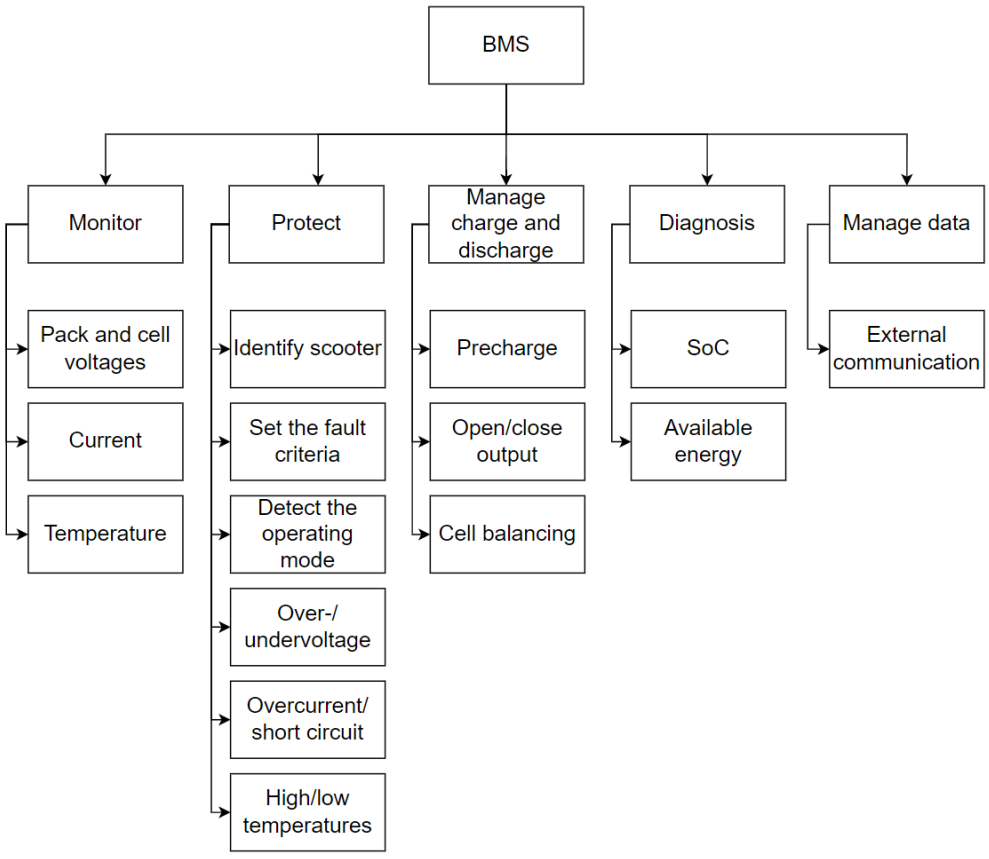


Figure 5. High-level diagram of BMS functionality. [3]

## 3.2 Schematics

The printed circuit board design, both schematics and layout, is done in KiCad which is an open-source electronics design software.

The most suitable BMS topology for the electric scooter battery pack is centralized topology due to its compactness and simplicity. That means only one PCB must be able to control the whole battery pack. Semi-distributed or distributed topology are used with higher number of cells when battery pack is divided into segments. Those topologies would add complexity to the system both hardware and software wise as the measurement data would be gathered from separate PCBs.

Hierarchical design is used in schematics instead of flat design so it would be easier to understand the overall work principle of the hardware (Figure 6). All the other sheets except “Power” are using wires and buses to connect to each other. “Power” schematic different voltage level inputs and outputs are global labels. That means they connect to the same label all over schematics without wire connection (marked green on Figure 6). This will keep the schematics cleaner with less signals and it is easier to read.

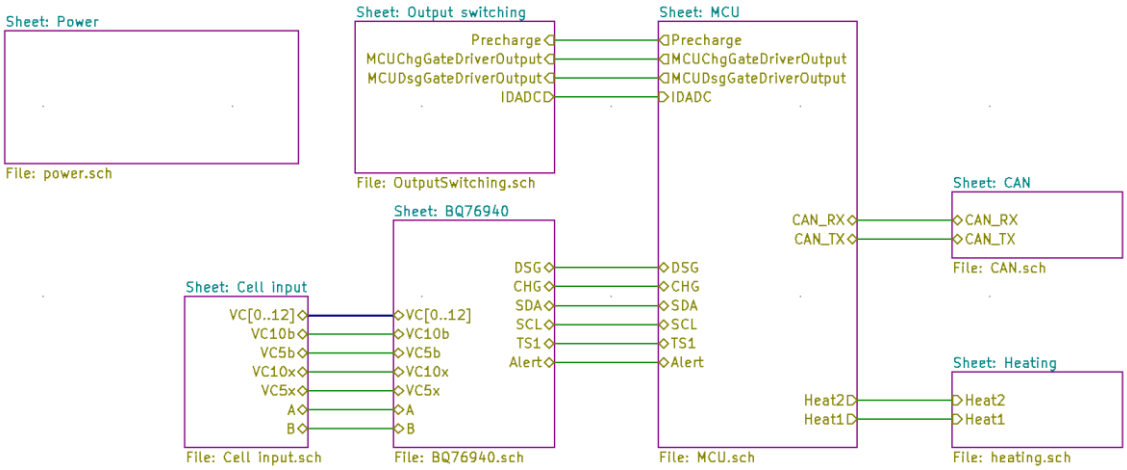


Figure 6. Hierarchical design of the BMS.

Microcontroller, marked with sheet name MCU, is controlling the BMS work. It communicates with the battery monitor BQ76940 which acquires voltage measurements from cells. The cell input sheet contains balancing circuits and low-pass filters. The MCU also controls the precharge and switching on the output of the battery pack. In addition,

it decides over the heating element usage and sends out necessary data via CAN bus which is the communication protocol used by the motor controller. The power sheet contains step-down switching regulator and low-dropout regulator to achieve voltage levels for different circuits.

### 3.2.1 Battery monitor

One of the most important parts of BMS design is the battery monitor IC. There is a variety of BMS IC-s on the market with different functionalities and factors that need to be considered before selecting the IC for a particular system. For example battery cell chemistry, maximum number of cells measured, balancing capability, protection features, sampling speed and accuracy, communication protocol etc.

As the aim of this thesis is to design a configurable battery management system, all analog BMS IC-s with preprogrammed limits were excluded because their limits cannot be changed. The IC needs to have a communication protocol to communicate with microcontroller. That is the easiest and most reasonable way to achieve configurable system. In addition, the BMS IC must fulfil the requirements listed in the second chapter "System requirements".

BQ76940 battery monitor IC, which is produced by Texas Instruments, was selected from electronic components distributor Digikey website [12] based on set requirements. It has two separate ADC-s. 14-bit ADC for cell voltages and temperature measurements and 16-bit ADC for current measurement. The IC could measure up to 15 cells with a variety of battery chemistries, including Li-ion. Battery pack monitoring (cell, current, temperature measurements), protection features and balancing are implemented through $I^2C$ protocol. Also, it has an alert pin to use with the host microcontroller with an interrupt signal to provide information about errors or that a new current measurement sample is available. To reduce the power consumption, different sub-blocks within the IC that can be disabled when not necessary. This is useful as the battery pack's energy is limited and reducing power consumption increases the scooters range. In addition, it has ship mode for ultra-low power state.

The ADC for voltage measurements can measure voltages up to 6,275 V in unsigned mode. With the resolution of 14 bits, the minimum step size can be calculated with the following formula (3.1).

$$V_x = \frac{V_{max}}{\mathrm{n}} = \frac{6{,}275\ \mathrm{V}}{2^{14}} = 382\ \mu\mathrm{V} \tag{3.1}$$

$V_x$ – step size, V

$V_{max}$ – full-scale range, V

n – ADC bits

The sampling rate of the BQ76940 for voltage and current measurements is 4 Hz and for temperature measurements 0,5 Hz. However, the overcurrent and short circuit protections are implemented using analog comparators with sampling frequency of 32 kHz. Current measurement is based on the shunt resistor and voltage drop is measured across it. The shunt resistor is R609 in the following figure (Figure 7). If the voltage drop measured on the resistor exceeds the programmed threshold, a configurable delay counter starts to count up. Upon reaching its value set in registry, error will be generated by updating a dedicated register value, pulling down the MOSFET gate driving pins CHG and DSG and switching ALERT pin high to inform the MCU of an error.

Resistors R603 and R604 are pull-up resistors for $I^2C$ signals. The REGSRC pin is the input of integrated LDO. The voltage regulator output (REGOUT) voltage is 3,3 V with this particular IC model used in schematics. As the maximum voltage of REGSRC is 36 V, there is a source follower circuit as suggested in the datasheet [13] before the pin to reduce the battery pack's voltage and not to exceed the maximum voltage of the pin. TS1-TS3 are temperature measurement connectors.

When selecting the shunt resistor value for current measurements, one has to consider using the maximum measurement range as well as keeping the overcurrent thresholds in suitable range without exceeding the maximum voltage ratings of the battery monitor. The IC has short circuit overcurrent protection threshold of maximum 0,2 V and the short circuit current is considered to be over 35 A. Maximum current peaks allowed when

accelerating with minimum voltage are below 35 A. The calculation for shunt resistor value is done with the well-known Ohms law as follows:

$$R = \frac{U}{I} = \frac{0{,}2\ V}{35} = 0{,}0057\ \Omega \tag{3.2}$$

R – shunt resistance, Ω

U – short circuit discharge threshold voltage, V

I – short circuit current, A

Considering tolerances, temperature coefficient and availability, 5 mΩ resistor is selected. The power rating of the resistor can be calculated

$$P = I^2 * R = 15^2 A * 0{,}005\ \Omega = 1{,}125\ W \tag{3.3}$$

P – power, W

I – maximum discharge current, A

R – shunt resistance, Ω

A shunt resistor with resistance of 5 mΩ is suitable with power rating bigger than 1,125 W to be able to handle continuous discharge power before interrupting the current flow.

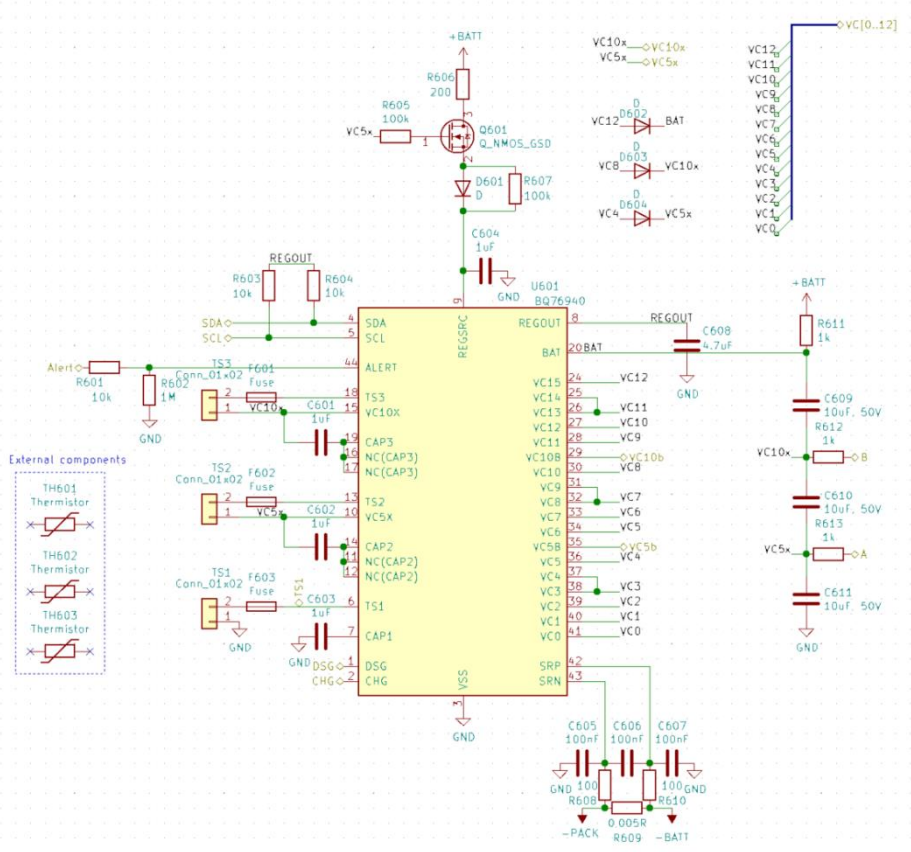


Figure 7. TI BQ76940 schematics.

### 3.2.2 Cell voltage measurement and balancing

Cell input schematics (Figure 8) consists of RC filter for every cell measurement, whereas the component value ranges were given in BQ76940 datasheet [13]. The passive balancing circuit consists of a P-channel MOSFET, a load resistor, a gate current limiting resistor and a zener diode. The balancing circuit driven by the BQ76940 when the host MCU has written specific balancing register values.

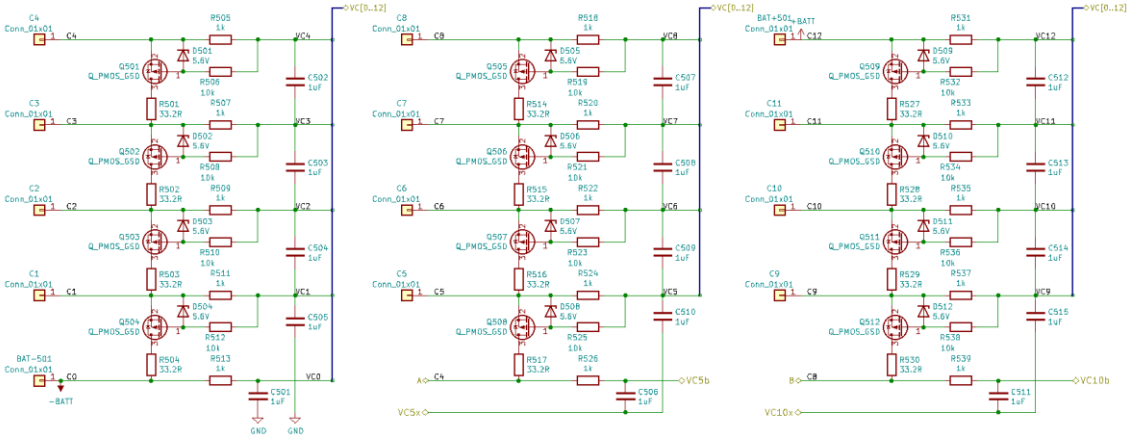

Figure 8. Cell input voltage measurement and balancing schematics.

### 3.2.3 Output switching and precharge

The output switching schematics (Figure 9) consist of voltage level shifter, gate driver, precharge circuit, output switching MOSFETs with diodes and two ESD protection diodes with capacitors.

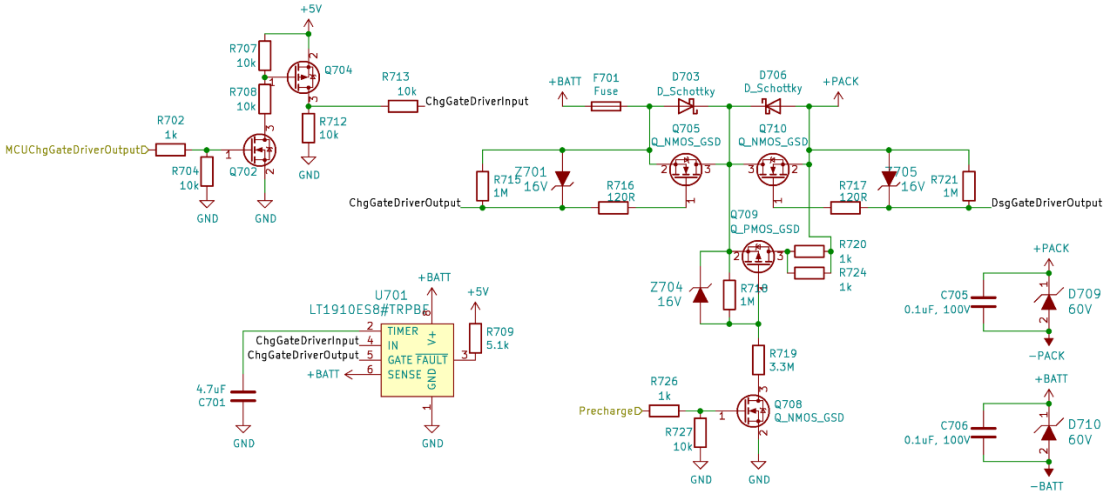

Figure 9. Output switching schematics.

The output switching MOSFETs are configured as a bidirectional switch because a single MOSFET can block the current in only one direction due to body diode. The chosen MOSFETs are N-channel due to their lower resistance compared to P-channel MOSFETs which decreases power losses and increases the efficiency. However, in high-side switching N-channel MOSFETs cannot be used without bootstrapping circuit or dedicated high-side gate driver with 100% duty cycle in this application.

That is because voltage applied to the N-channel MOSFET gate, with reference to source, needs to be higher at least the threshold value to go to closed state without exceeding the maximum gate voltage rating. The gate-source threshold voltage is in low-side configuration with reference to ground. However, when the N-channel MOSFET is used in high-side application and the MOSFET goes to closed state, the source voltage becomes equal to drain voltage and the gate voltage is not enough to keep the MOSFET closed. Therefore the gate voltage must be at least source voltage + gate threshold voltage.

LT1910, produced by Linear Technology Inc, was selected to the schematics which is a high-side gate driver designed for N-channel power MOSFETs for high-side switching applications with 100% duty cycle.

The precharge circuit switches the P-channel MOSFET to closed state and the inverter's DC link capacitor will be charged through precharge resistors R720 and R724. The maximum precharge resistor value can be calculated with the following formula when maximum precharge time (in this case 2 seconds) is set to get almost fully (99,33%) charged capacitor:

$$R_{max} = \frac{5\mathrm{T}}{C} \tag{3.4}$$

$R_{max}$ – maximum precharge resistor resistance, **Ω**
T – time constant, s
C – capacitor capacitance, F

As the voltage rise on the capacitor is exponential, the increase is faster in the beginning and then it flattens as the capacitor gets more charged. The voltage on the capacitor can be calculated with the following formula:

$$V_C(t) = V_s\left(1 - e^{-\frac{t}{RC}}\right) \tag{3.5}$$

$V_C$ – voltage across the capacitor, V
$V_S$ – battery pack voltage, V
e – Euler's number

t – time, s

R – precharge resistor resistance, Ω

C – capacitor capacitance, F

As the voltage difference between four (4T) and five time constants (5T) is rather small (Figure 10) and steady state is achieved, 4T is preferred to select a resistor with smaller resistance and therefore faster precharge. The maximum precharge resistor value can is calculated as follows:

$$R = \frac{4\tau}{C} = \frac{4 * 0{,}4\ s}{0{,}003\ F} = 533{,}33\ \Omega \tag{3.6}$$

R – precharge resistor resistance, Ω

T – time constant, s

C – capacitor capacitance, F

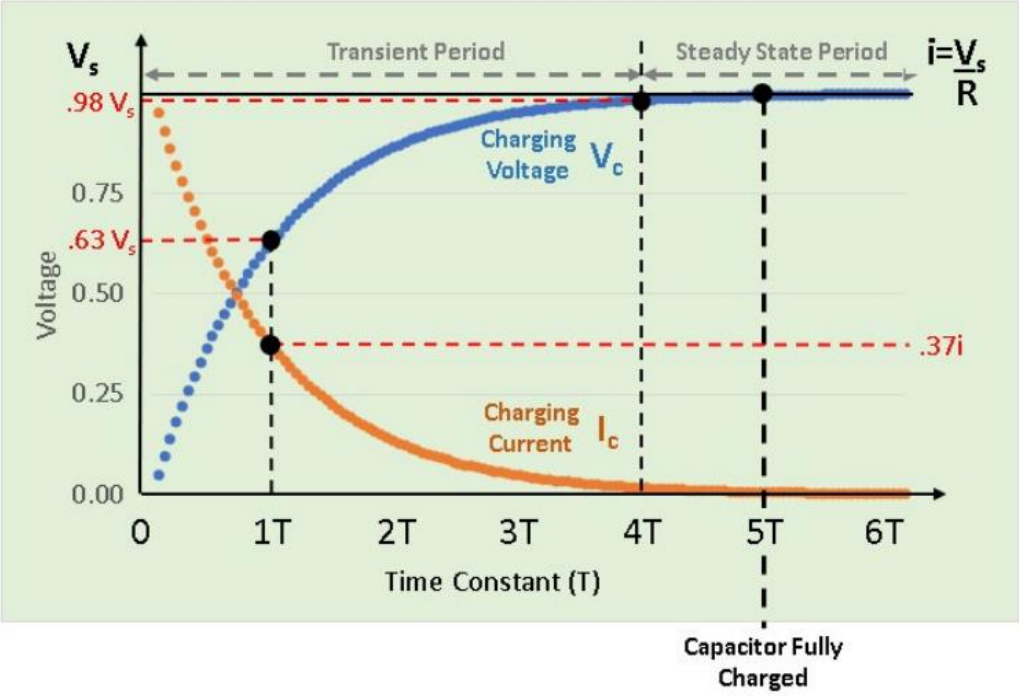


Figure 10. Precharge voltage and current vs time plot [14].

The resistors power rating should be selected so that it could handle maximum precharge power constantly in case output is not switching to closed state. Maximum power occurs at the beginning of precharge when the capacitor is at 0 V. The maximum power can be calculated:

$$P = \frac{U^2}{R} = \frac{50{,}4^2\ V}{533{,}33\ \Omega} \approx 4{,}7\ W \tag{3.7}$$

P – power, W

U – voltage, V

R – resistance, Ω

Two 1 kΩ resistors (R720 and R724 in Figure 9) with power rating of 3 W are placed in parallel to fulfil the requirements.

The output switching MOSFETs and diodes allow the system to use only charging or only discharging or both charging and discharging modes. Allowing only charging is useful to protect the battery when the SoC of the battery pack is so low that the minimum voltage threshold has been exceeded and no more discharge can be allowed.

According to the datasheet [15], the chosen MOSFET has maximum drain-source on-state resistance 0,0017 Ω while the gate-source voltage is at least 10 V. Maximum junction-to-ambient thermal resistance ($R_{thJA}$) is 20 °C/W and maximum operating temperature is 150 °C. Therefore the maximum power dissipation without additional cooling or heat sinks is 6,25 W at ambient temperature of 25 °C.

$$P = \frac{T_{jmax} - T_{ambient}}{R_{thJA}} = \frac{150\ °\text{C} - 25\ °\text{C}}{20\ °\text{C/W}} = 6{,}25\ W \tag{3.8}$$

P – power, W

$T_{jmax}$ – maximum junction operating temperature, °C

$T_{ambient}$ – ambient temperature, °C

$R_{thJA}$ – maximum junction-to-ambient thermal resistance, °C/W

The continuous drain current exceeds 40 A which is more than enough in this application as short circuit is considered to be over 35 A. The source-drain diode forward voltage is approximately 0,8 V at 25 A and 25 °C. The maximum continuous source-drain current can be calculated 6,25 W / 0,8 V ≈ 7,8 A. With lower current the forward voltage is even

lower and therefore the current should be higher. However, in the datasheet the maximum continuous source-drain diode current with ambient temperature 25°C is stated to be 5,6 A. To avoid exceeding the maximum power ratings, three MOSFETs are placed in parallel on schematics, but not all of them will be soldered.

To increase the efficiency and save the MOSFETs from unnecessary heat dissipation, three Schottky diodes will be added parallel to the MOSFET body diodes. The chosen diode [16] has a maximum operating junction temperature 150 °C and typical thermal resistance 55 °C/W in free air with ambient temperature of 25 °C. The maximum power dissipation is calculated to be 2,27 W. The forward voltage with 5 A is 0,42 V. This is within the continuous power limits of the diode. With three MOSFET body diodes and three Schottky diodes the maximum continuous current is approximately 30 A which is with margin of safety and should not be reached with normal operation of the scooter.

There are transient-voltage-suppression (TVS) diodes and capacitors before and after the MOSFETs to avoid transient voltages and electrostatic discharge (ESD) when assembling the battery pack to the PCB or when connecting the output connector.

### 3.2.4 Microcontroller

When selecting the MCU, previous experience with STMicroelectronics MCUs was considered. As the battery pack's energy is limited and the BMS power consumption should be as low as possible, ultra-low-power series is suitable. The MCU needs at least 4 ADC, 1 interrupt and 8 general purpose input/output (GPIO) pins. In addition, it needs $I^2C$ connectivity to be able to communicate with battery monitor IC BQ76940 by Texas Instruments and CAN connectivity to communicate with motor controller. Based on the requirements and availability, STM32L552ZCT6 was chosen. It has all the necessary peripherals and LQFP case that is useful while prototyping because of easy soldering. Ideally a MCU with less than 144 pins would have been selected to save space and fasten the soldering process, but due to a lack of microcontrollers on the market because of global chip shortage that started with COVID-19, there were not too many alternatives to choose from.

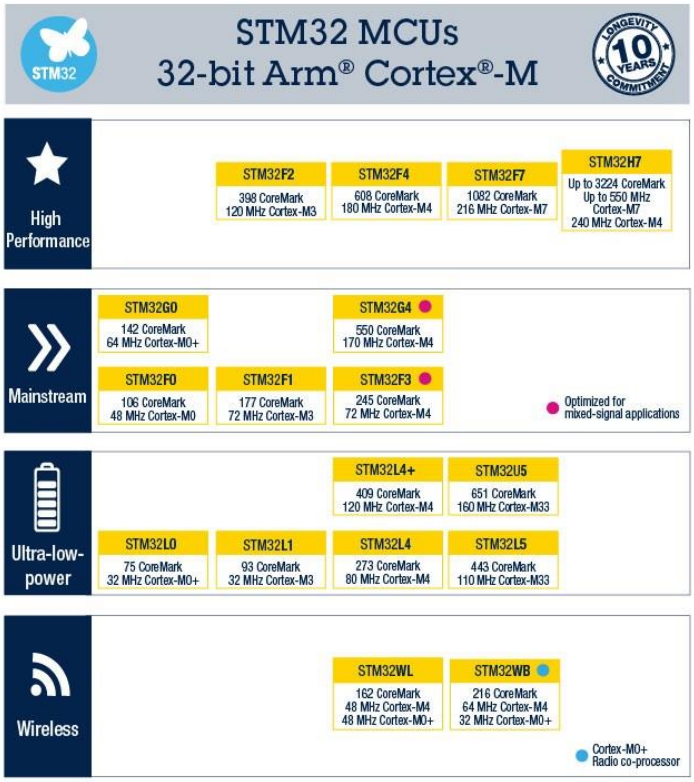


Figure 11. STM32 microcontroller series [17].

Given the working environment of BMS, an external crystal oscillator is chosen for providing clock source for CPU and peripherals. These kinds of oscillators are more accurate compared to internal oscillator found inside the MCU, which contributes to better real-time performance of program execution. Another advantage of external crystal oscillators is that fluctuations in ambient temperature do not affect their operating frequency as much compared to internal RC oscillators [18].

On a PCB, where low power consumption is important, unused MCU pins should not be left floating. They should be either pulled down to PCB ground or pulled up to MCU supply voltage, because noise on floating input pin could result in increased power consumption. As mentioned in the STMicroelectronics application note AN4899 [19], unconnected pins have been pulled to ground to improve protection against electrostatic discharge.

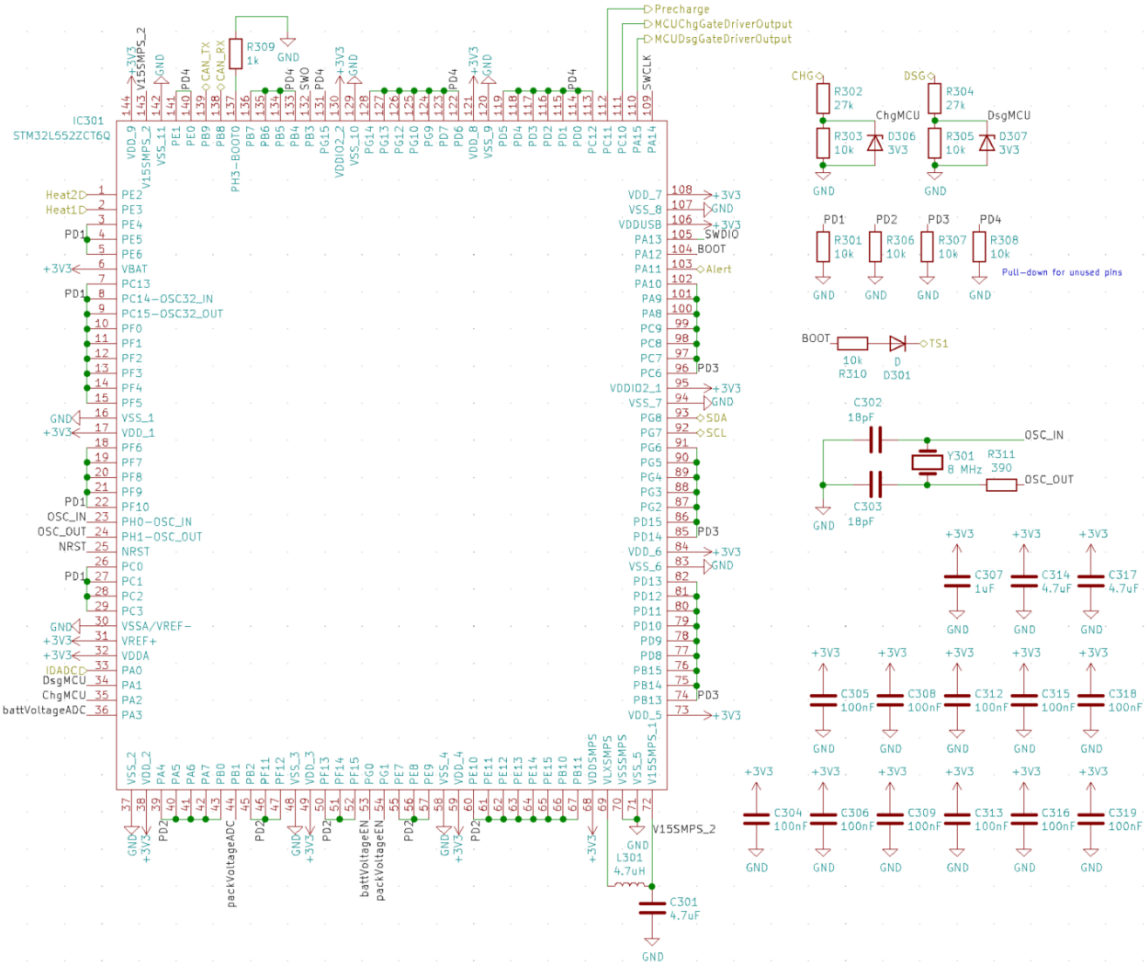


Figure 12. MCU schematics.

### 3.2.5 Power schematics

For power schematics design (Figure 13) there was calculated estimated simplified power consumption based on the best- and worst-case scenarios in terms of power consumption of different ICs which can be seen below (Table 3).

**Table 3. Simplified estimated power consumption.**

| Component | Min [W] | Max [W] |
|---|---|---|
| BQ76940 [13] | 0,004 | 0,018 |
| STM32L552 [20] | 0,000003 | 0,056 |
| MCP2551 [21] | 0,002 | 0,062 |
| LT1910 [22] | 0,058 | 0,178 |
| Total | 0,064 | 0,314 |

The power input for the PCB comes from the battery cells and is in range of 36-50,4 V. There are two necessary voltage levels needed for the ICs: 5 and 3,3 V. For 5 V output LT8618 is used which is a step-down switching regulator made by Analog Devices. Low-dropout regulator with an input of 5 V is used for 3,3 V output.

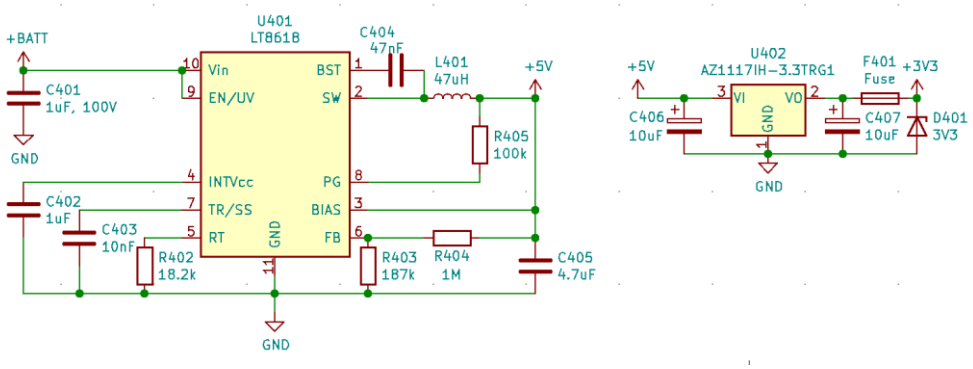


Figure 13. Power schematics.

## 3.3 Layout

The PCB has two signal layers and all the components are placed on the top side. This will make debugging easier as it is more convenient to measure voltages across components when necessary. In addition, six test points were added on the top side to quicken the testing process.

Another important principle of the layout design was to keep the high current signals away from the rest of the system – the measurement circuits and filters, different ICs etc. It is recommended in the BQ76940 datasheet [13] to avoid interferences (Figure 14). The ground is the same for the low and high current circuits, but they are interconnected through a 0 Ω resistor.

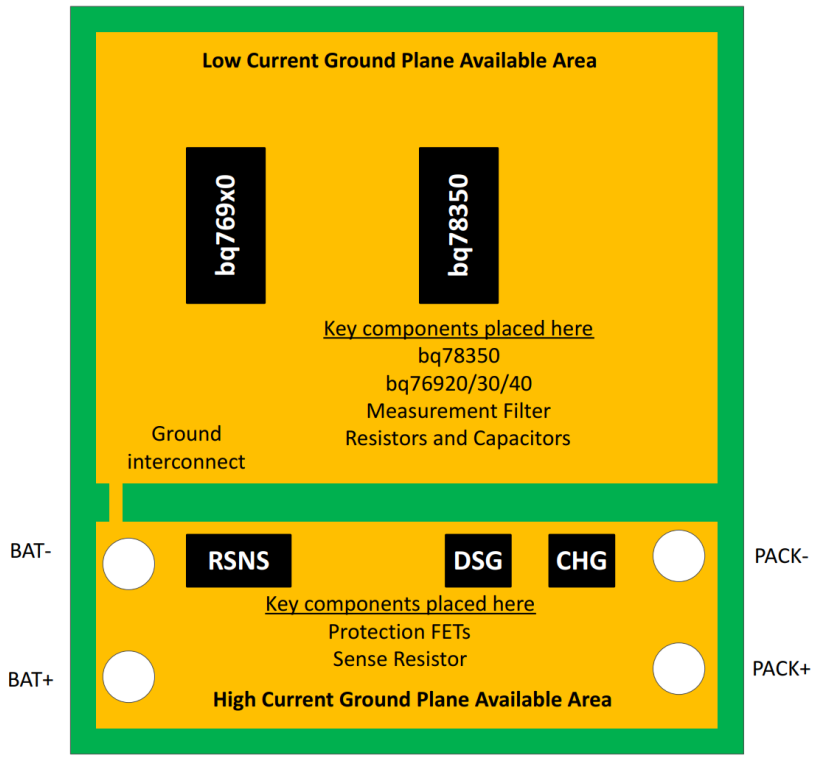


Figure 14. Layout guideline from BQ76940 datasheet [13].

The rest of the layout was divided into sub-blocks after separating high and low current circuits. The sub-blocks are marked with different colour in the following figure (Figure 15):

- red – high current
- orange – heating pad outputs
- yellow – MCU with external oscillator and programming connector
- green – CAN bus
- brown – BQ76940
- purple – gate drivers
- blue – voltage regulators
- gray - precharge

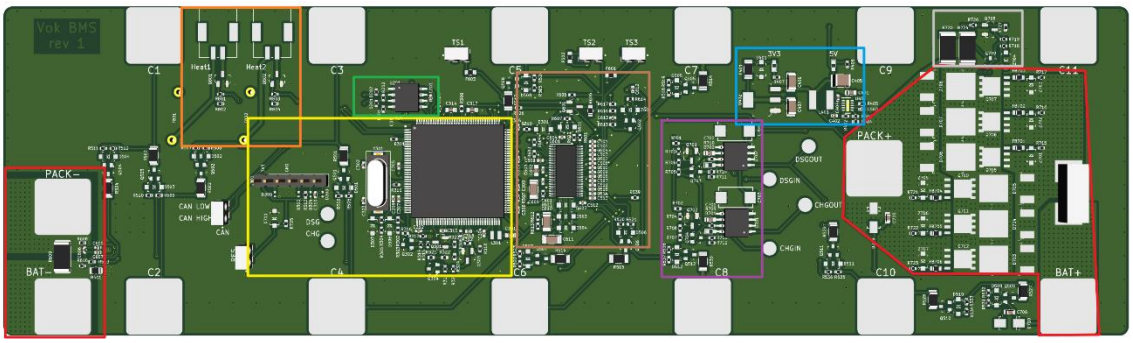


Figure 15. Top side of the layout.

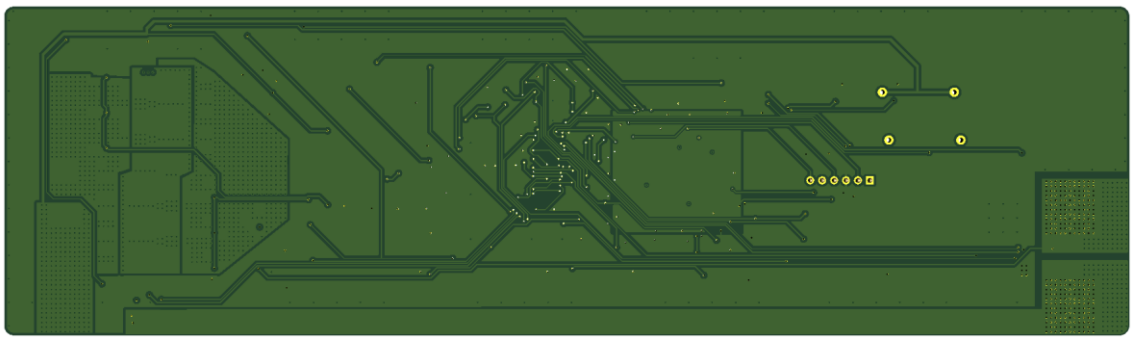

Figure 16. Bottom side of the layout.

To improve thermal properties, through hole vias are introduced to the circuit board (Figure 17). These are holes made into the PCB specifically for heat transfer via air - that is called convection. Buried vias and microvias are preferred to lower the thermal resistance even more. The thermal resistance with and without microvias and buried vias can differ more than 30 times [23]. However, buried vias and microvias add cost to the manufacturing.

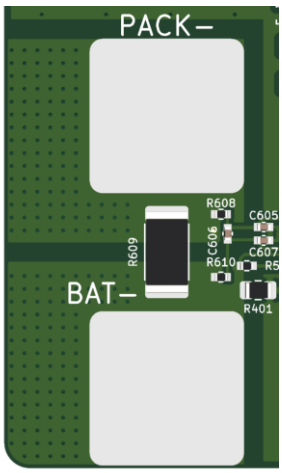


Figure 17. Thermovias placed near the pads in high current path.

# 4 Software

For MCU programming the STM32CubeIDE (Figure 18) is used which is an C/C++ development platform for STM32 MCUs. Its main benefit is code generation based on peripheral configuration for selected microcontroller. The engineer can focus on the configuration itself in a graphical environment rather than configuring MCU registers manually which tends to be a considerably time-consuming process.

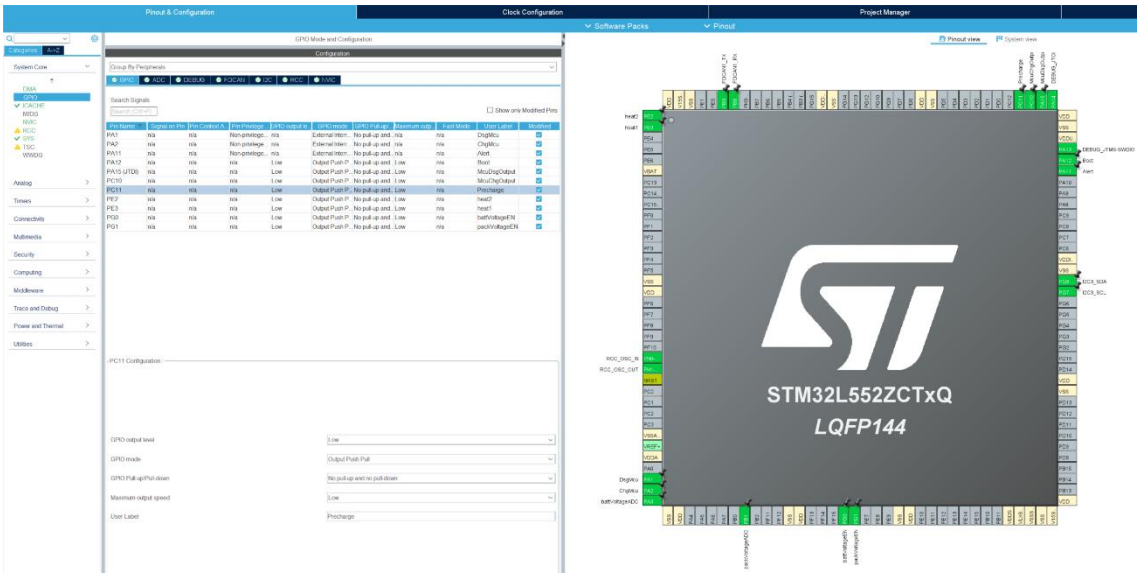


Figure 18. STM32CubeIDE development platform.

Chosen MCU is programmed using a debugger device called ST-Link. This device is provided by STMicroelectronics. Chosen interface for connecting the debugger with target device is serial wire debug (SWD). This connection uses 5 wires in total and provides sufficient debugging capabilities. It lets the user place breakpoints, enter functions, view values of variables in real time etc.

## 4.1 Program code/firmware

Program code for BMS consists of application specific code and peripheral drivers which have been generated using STM32CubeIDE environment. Program flow has been depicted in the following figure (Figure 19). It can be seen that after MCU has booted, it starts initializing peripherals and user written functions. After that endless while loop is entered and application specific functions are being executed. Most of the functions are

periodic which means they are executed after certain time has been passed. There is a timing system implemented in the code which increments a counter every time a system clock based hardware timer calls an interrupt. This timing system is used to check whether enough time has passed to execute corresponding functions.

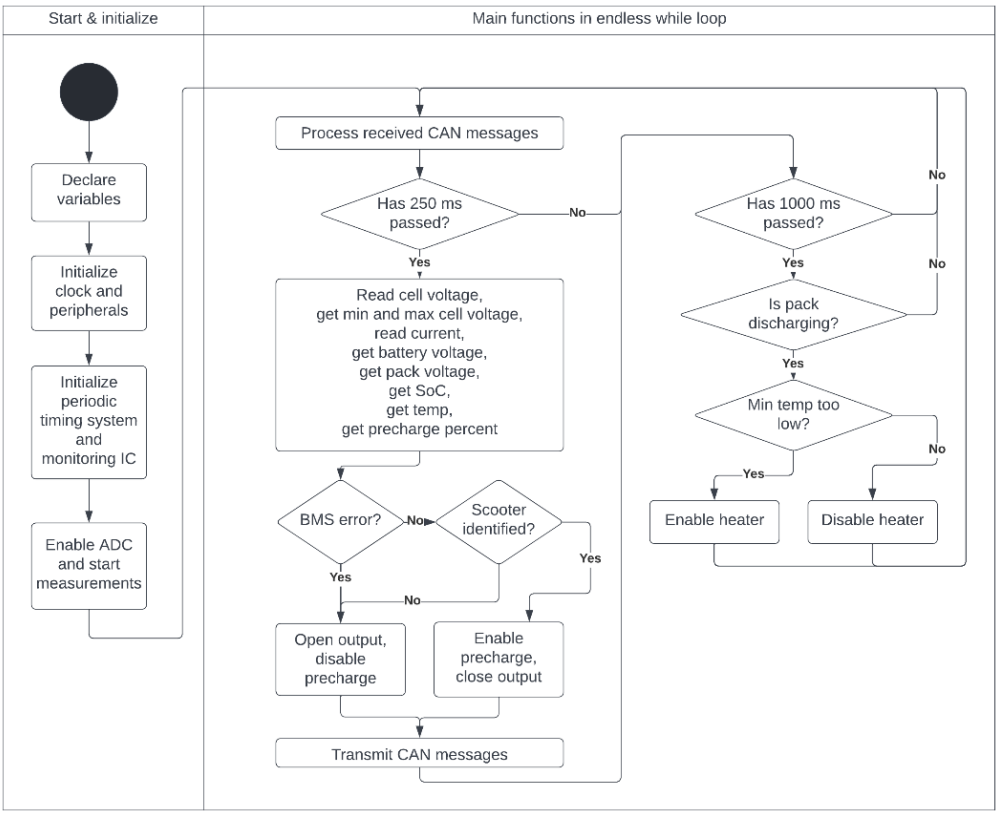


Figure 19. Firmware UML diagram.

### 4.1.1 Interfacing with BQ76940 monitoring IC

When powering up the BQ76940 device, it needs to be configured to start normal operation. This means certain registers of the IC have to be written with user specified values. Register map with required explanations is given in BQ76940's datasheet [13]. First, cell balancing is turned off by writing 0x00 values in corresponding registers. After that using SYS_CTRL1 register, ADC readings of temperature and voltage are enabled together with activating the use of external thermistors for measurement. SYS_CTRL2 register is configured to enable continuous current monitoring with coulomb counter. Next, registers which protect the IC are configured. Short circuit in discharge delay time is set to 100 µs and overcurrent in discharge delay time to 320 ms. Undervoltage delay

time is programmed to 2 s and overvoltage delay time to 2 s. ADC gain registers are read and values used in calculating the actual gain of ADC which becomes necessary later in the program code where real voltage and temperature values are calculated.

### 4.1.2 Important functions

- Read cell voltage – BQ76940 has two registers for each cell which hold the result of cell voltage value. Bit-shifting is used to add corresponding content from both registers together to obtain raw reading. After that considering previously calculated ADC gain value, the actual cell voltage is calculated.

- Get minimum and maximum cell voltages – this function finds minimum cell voltage, maximum cell voltage and stores their location in battery pack. Additionally it generates an error when a cell has too low or too high voltage.

- Read current – coulomb counter registers are used to read values and calculate battery pack current. Depending whether current value is negative or positive, battery pack discharging or charging state can be determined. An error is generated when discharging or charging currents exceed safe limits.

- Get battery voltage – this function is used to calculate the voltage of whole battery pack.

- Get pack voltage – this function measures the voltage on the output

- Get SoC – State of charge of the whole battery pack is calculated as a percentage. This could be used for indicating battery charge levels.

- Get temperatuure – values read from two registers are used to find temperature reading. In total 3 different temperature readings are made. Minimum and maximum values are found. If temperature value is out of safe range, an error is generated.

- Get precharge percent – this functions gives the percentage value of precharge

# 5 Testing

Based on the V-model that was described in chapter 3 “Hardware design” the testing process started with software testing. Firstly, ADCs and GPIOs were tested, followed by $I^2C$ and CAN bus testing. Once these functionalities were working as expected it was time to move on with testing different sub-systems such as cell voltage readings with BMS IC or precharge and output MOSFETs switching for example.

## 5.1 Measurements

### 5.1.1 Cell voltage measurements

Digital multimeter Metrahit 27I was used to check the BQ76940 measurements. This multimeter is produced by Gossen Metrawatt. The resolution of the multimeter was at 1 mV and the uncertainty was ± 0,1 % of the reading + 5 digits according to the datasheet [24]. The BQ76940 has the resolution of 1 mV and ADC cell voltage accuracy of ± 10 mV at 25 °C according to its datasheet [13]. Cell voltage measurements with the BQ76940 and Metrahit 27I are compared in the following table (Table 4).

**Table 4. Cell voltage measurements.**

| | Metrahit 27I [mV] | BQ76940 [mV] | Difference [mV] |
|---|---|---|---|
| Cell 1 | 3761 ± 8,761 | 3773 ± 10 | -12 |
| Cell 2 | 3763 ± 8,763 | 3779 ± 10 | -16 |
| Cell 3 | 3763 ± 8,763 | 3776 ± 10 | -13 |
| Cell 4 | 3762 ± 8,762 | 3771 ± 10 | -9 |
| Cell 5 | 3762 ± 8,762 | 3773 ± 10 | -11 |
| Cell 6 | 3761 ± 8,761 | 3773 ± 10 | -12 |
| Cell 7 | 3763 ± 8,763 | 3774 ± 10 | -11 |
| Cell 8 | 3761 ± 8,761 | 3768 ± 10 | -7 |
| Cell 9 | 3765 ± 8,765 | 3773 ± 10 | -8 |
| Cell 10 | 3764 ± 8,764 | 3774 ± 10 | -10 |
| Cell 11 | 3765 ± 8,765 | 3777 ± 10 | -12 |
| Cell 12 | 3762 ± 8,762 | 3769 ± 10 | -7 |

The minimum voltage difference was 7 mV while the maximum was 16 mV. The average difference was approximately 10,6 mV. However, both measurements overlap in the uncertainty range. In worst case scenario with 16 mV difference the Metrahit 27I measurement would be 3763 ± 8,763 mV and for the BQ76940 3779 ± 10 mV.

### 5.1.2 CAN messages and periodic task execution

Kvaser CanKing software was used with Kvaser Leaf Light HS v2 [25] universal serial bus (USB) to CAN adapter to check communication. CAN database was formed with Kvaser Database Editor to ease the debugging process. The database can be imported to CanKing and the CAN messages are displayed as in the following picture. The messages and signals will have a dedicated name, the values can have factor and offset if needed, proper units and value definition can be implemented.

| Identifier | Flg | Dlc | Name | | | Time | Dir |
|---|---|---|---|---|---|---|---|
| 00000100 | | 8 | bms.can_transmit | | | 49.337170 | R |
| | | | -> errorState | 0.0000 | | | |
| | | | -> SoC | 82.0000 | % | | |
| | | | -> packState | 0.0000 | | | |
| | | | -> prechargePercent | 0.0000 | % | | |
| 00000101 | | 8 | bms.can_transmit2 | | | 49.337340 | R |
| | | | -> minTemp | 24.0000 | *C | | |
| | | | -> maxTemp | 24.0000 | *C | | |
| | | | -> packPower | 0.0000 | W | | |
| | | | -> packVoltage | 45.8700 | V | | |
| | | | -> packCurrent | 0.0000 | A | | |
| 00000102 | | 8 | bms.can_transmit3 | | | 49.337420 | R |
| | | | -> avgCellVoltage | 3782.0000 | mV | | |
| | | | -> minCellVoltage | 3777.0000 | mV | | |
| | | | -> maxCellVoltage | 3788.0000 | mV | | |
| | | | -> minCellLocation | 7.0000 | | | |
| | | | -> maxCellLocation | 1.0000 | | | |

Figure 20. CAN messages.

CAN message transmission function was used to measure the periodic task execution time in the while loop of the program code (Figure 19). The CAN transmission execution should take place every 250 ms or in other words with frequency of 4 Hz. The task execution period was measured with Kvaser CanKing and Kvaser Leaf Light HS v2 (Figure 21). The difference between the measured and expected scheduling period is below 0,03%. This is acceptable error in this application and no further analysis was conducted.

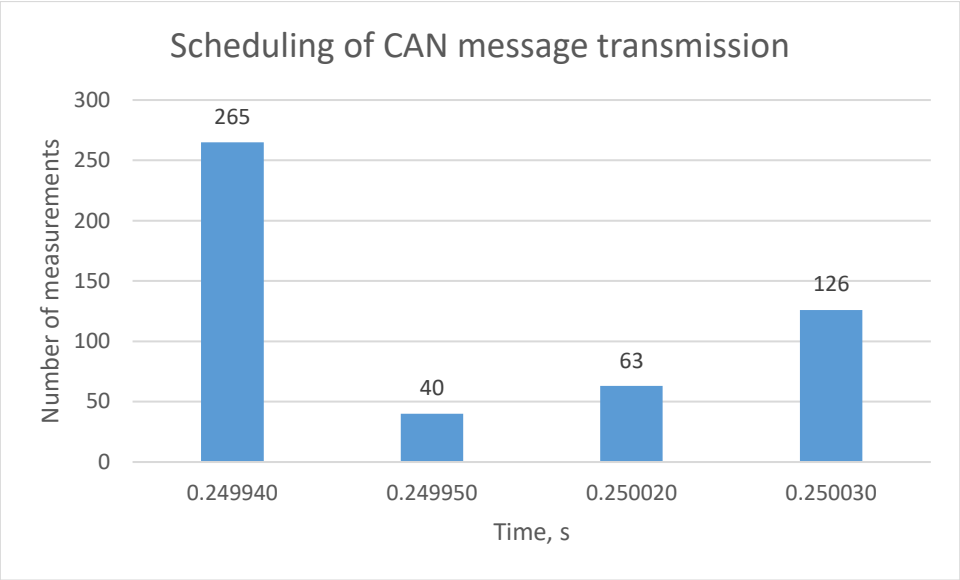


Figure 21. Task execution timing measurements based on CAN message transmission.

### 5.1.3 Output switching schematics prototype

Before starting with the PCB layout, the concept of bidirectional MOSFET switch with dedicated high-side gate driver was tested with breadboard and a custom PCB. The gate driver LT1910 with additional resistors and a capacitor was attached to the breadboard. The power MOSFETs, diodes and a fuse were soldered to a custom PCB due to their surface mount device (SMD) footprints. Both charging and discharging current directions were tested and the schematics was verified to be used on a real board as well.

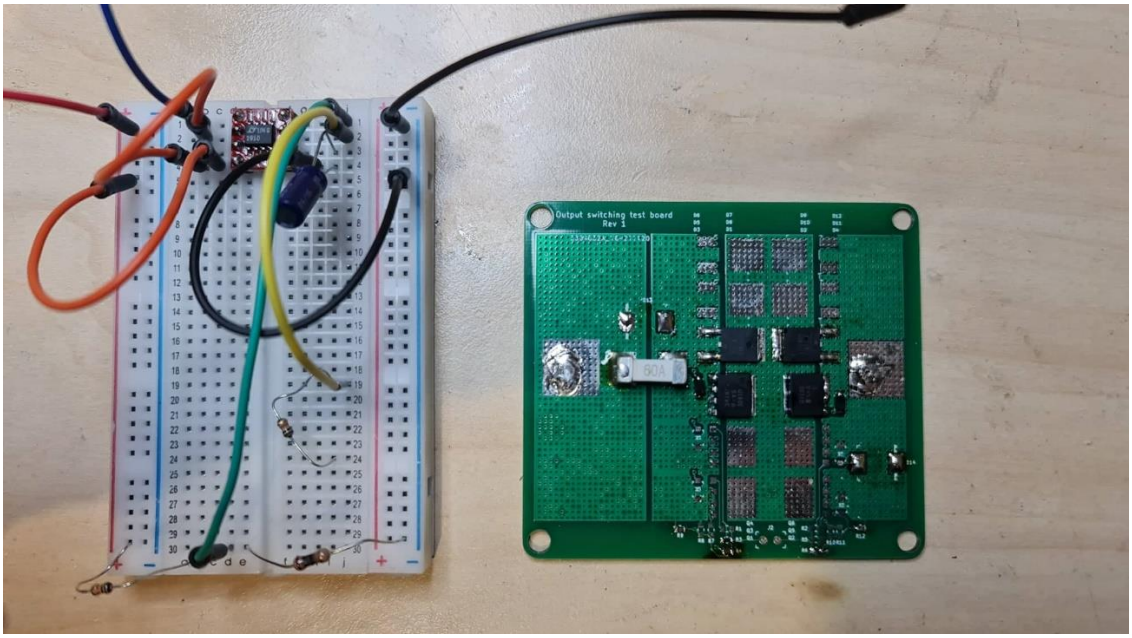


Figure 22. Breadboard with LT1910 on a breakout board and bidirectional MOSFET switch prototype.

### 5.1.4 Precharging

Precharging was measured with an oscilloscope while the battery pack output was connected to the motor controller (inverter). No other loads were connected. The inverter's DC link capacitance is 2,04 mF, the precharge resistance is 500 Ω, the supply voltage is 47,3 V and the output MOSFETs are closed upon precharge is reaching 90% of supply voltage.

According to the capacitor voltage charge formula (3.5) the time to reach 90% or 42,6 V precharge is approximately 2,35 seconds. However, the measured value is 2 seconds (Figure 23). This is because diodes and MOSFETs have reverse voltage leakage current. The diode datasheet [16] states that the maximum reverse current is 5 mA with reverse voltage of 60 V at 25 °C. The MOSFETs have maximum zero gate voltage drain current 1 µA.

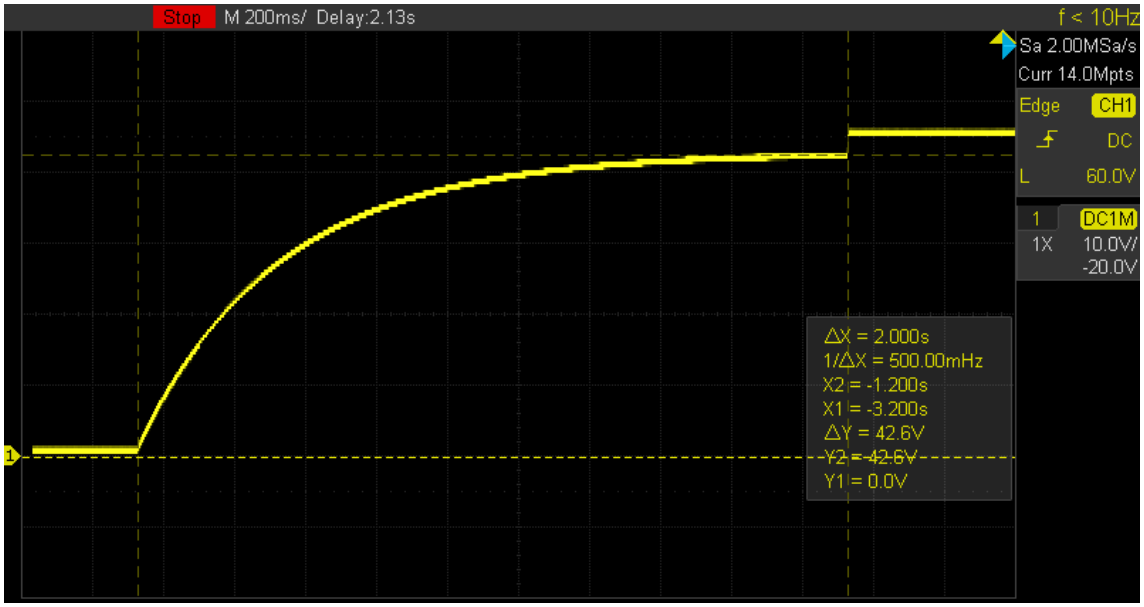


Figure 23. Precharge measurement with oscilloscope.

The diodes reverse current impact on precharge can be simplified into parallel resistance with existing precharge resistor. MOSFETs zero gate voltage drain current will not be considered as it is significantly smaller. With the 47,3 V supply and 500 Ω precharge resistance value the maximum current is 94,6 mA. Three diodes reverse current is approximately 15 mA. The total maximum precharge current is therefore approximately 109,6 mA. Calculating the resistance value with taking into account the diodes is 47,3 V

/ 109,6 mA ≈ 431,5 Ω. When applying this resistance value into equation (3.5 the calculated precharge time is ~ 2,03 s which is nearly the same as in oscilloscope's graph (Figure 23).

# 6 Summary

The aim of the thesis was to design a user programmable battery management system for an electric scooter that would protect the scooter's battery pack with user set and programmed voltage, current and temperature limits. The expected results shall be confirmed with testing.

Firstly, different products with similar purpose on the market were compared and analysed to get an overview. Problematic areas were defined and after that system concept was planned and requirements were set. Hardware design started with schematics design and calculations, followed by printed circuit board layout design. Software architecture and working principles was introduced. First revision of the design got tested and the conclusion could be drawn.

As a results the battery management system worked in general as designed without bigger drawbacks. The user can programm the safety limits of the system and the BMS keeps the battery pack. The future work could improve and optimize the design in terms of both hardware and software.

In terms of software, more accurate but also more complex SoC algorithm could be used to estimate the driving range more precisely. Pack discharge cycle count could be stored into the MCU memory to keep track of the battery pack usage and aging. MCU and battery monitor IC could be used in sleep mode while the battery pack is not in use to reduce power consumption.

Hardware could be optimized to reduce the power consumption even more by removing unnecessary components from the schematics that do not affect the performance of the system.

# References


[1] Z. Wang, J. Yuan, X. Zhu, H. Wang, L. Huang, Y. Wang and S. Xu, "Overcharge-to-thermal-runaway behavior and safety assessment of commercial lithium-ion cells with different cathode materials: A comparison study," *Journal of Energy Chemistry*, pp. 484-498, 21.07.2020.

[2] W. Chen, J. Jiang and J. Wen, "Thermal runaway induced by dynamic overcharge of lithium-ion batteries under different environmental conditions," *Journal of Thermal Analysis and Calorimetry*, pp. 855-863, 22.07.2020.

[3] C. Fleischer, J. V. Barreras, D. U. Sauer, E. Schaltz and A. E. Christensen, "Development of Software and Strategies for Battery Management System Testing on HIL Simulator", 2016. [Online]. Available: https://www.researchgate.net/publication/322477987_Development_of_software_and_strategies_for_Battery_Management_System_testing_on_HIL_simulator. [Accessed 12.10.2021].

[4] W. J. T., Lithium-Ion Battery Chemistries: A Primer, Amsterdam: Elsevier, 2019.

[5] G. Graber, "Electric Mobility: Smart Transportation in Smart Cities," 2016. [Online]. Available: https://www.researchgate.net/publication/303629402_Electric_Mobility_Smart_Transportation_in_Smart_Cities?channel=doi&linkId=574ab0ab08ae5f7899ba00ba&showFulltext=true. [Accessed 17.04.2022].

[6] "Inductor Selection Guide for BMS Battery Management System," [Online]. Available: https://passive-components.eu/bms-battery-management-system-explained-and-inductor-selection-guide/. [Accessed 12.01.2022].

[7] D. Bokma, "DieBieMS - Hardware, GitHub," [Online]. Available: https://github.com/DieBieEngineering/DieBieMS. [Accessed 06.12.2021].

[8] K. Dionne, "ENNOID-BMS GEN1," [Online]. Available: https://www.ennoid.me/bms/gen-1. [Accessed 06.12.2021].

[9] "Daly DL15S," [Online]. Available: https://www.aliexpress.com/i/4000812857743.html. [Accessed 06.12.2021].

[10] "LG INR18650HG2 datasheet," 28.01.2015. [Online]. Available: https://www.batteryspace.com/prod-specs/9989.specs.pdf. [Accessed 12.02.2022].

[11] S. Ma, M. Jiang, P. Tao, C. Song, J. Wu, J. Wang, T. Deng and W. Shang, "Temperature effect and thermal impact in lithium-ion batteries: A review," *Progress in Natural Science: Materials International*, vol. 28, no. 6, pp. 653-666, 12 2018.

[12] "Digikey website," [Online]. Available: https://www.digikey.com/. [Accessed 30.01.2022].

[13] Texas Instruments, "BQ76940 datasheet," [Online]. Available: https://www.ti.com/lit/ds/symlink/bq76940.pdf?ts=1641934568732&ref_url=https%253A%252F%252Fwww.google.co.il%252F. [Accessed 02.12.2021].

[14] B. Munari and A. Schneer, “How to design a precharge circuit for hybrid and electric vehicle applications,” 12.11.2020. [Online]. Available: https://www.sensata.com/sites/default/files/a/sensata-how-to-design-precharge-circuits-evs-whitepaper.pdf. [Accessed 17.04.2022].

[15] “SiDR626DP datasheet,” 01.01.2022. [Online]. Available: https://www.vishay.com/docs/75748/sidr626dp.pdf. [Accessed 17.02.2022].

[16] “V35PW60 datasheet,” 01.01.2022. [Online]. Available: https://www.vishay.com/docs/87687/v35pw60.pdf. [Accessed 17.02.2022].

[17] “STM32 32-bit Arm Cortex MCUs,” [Online]. Available: https://www.st.com/en/microcontrollers-microprocessors/stm32-32-bit-arm-cortex-mcus.html. [Accessed 08.04.2022].

[18] E. Corpeño, “The Good and the Bad of MCU Internal Oscillators,” 11.12.2019. [Online]. Available: https://www.allaboutcircuits.com/technical-articles/the-good-and-the-bad-of-mcu-internal-oscillators/. [Accessed 10.04.2022].

[19] “STM32 microcontroller GPIO hardware settings,” 29.03.2022. [Online]. Available: https://www.st.com/resource/en/application_note/an4899-stm32-microcontroller-gpio-configuration-for-hardware-settings-and-lowpower-consumption-stmicroelectronics.pdf. [Accessed 15.04.2022].

[20] STMicroelectronics, “STM32L552 datasheet,” [Online]. Available: https://www.st.com/resource/en/datasheet/stm32l552zc.pdf. [Accessed 25.03.2022].

[21] M. T. Inc., “MCP2551 datasheet,” [Online]. Available: http://ww1.microchip.com/downloads/en/devicedoc/20001667g.pdf. [Accessed 25.03.2022].

[22] L. T. Corporation, “LT1910 datasheet,” [Online]. Available: https://www.analog.com/media/en/technical-documentation/data-sheets/1910fc.pdf. [Accessed 10.04.2022].

[23] B. Heinz, “Heat management of circuit boards,” [Online]. Available: https://www.we-online.com/web/en/index.php/show/media/04_leiterplatte/2011_2/relaunch/produkte_5/heatsink/neu_2011/TecReport_01_2011_EN_S.pdf. [Accessed 12.02.2022].

[24] “Gossen Metrawatt Metrahit 27I datasheet,” [Online]. Available: https://www.gmc-instruments.de/media/doku/tx/metrahit-27/metrahit-27-db_gb.pdf. [Accessed 15.04.2022].

[25] Kvaser, “Kvaser Leaf Light HS v2 datasheet,” [Online]. Available: https://canlandbucket.s3-eu-west-1.amazonaws.com/productionResourcesFiles/bd3328ef-9712-452c-94c0-e61a875adade/73-30130-00685-0_EN.pdf. [Accessed 20.04.2022].

# Appendix 1 – Non-exclusive licence for reproduction and publication of a graduation thesis[1]

I Kristjan Kõuts

1. Grant Tallinn University of Technology free licence (non-exclusive licence) for my thesis “Development of a User Programmable Battery Management System for an Electric Scooter”, supervised by Kaiser Pärnamets
   1.1. to be reproduced for the purposes of preservation and electronic publication of the graduation thesis, incl. to be entered in the digital collection of the library of Tallinn University of Technology until expiry of the term of copyright;
   1.2. to be published via the web of Tallinn University of Technology, incl. to be entered in the digital collection of the library of Tallinn University of Technology until expiry of the term of copyright.
2. I am aware that the author also retains the rights specified in clause 1 of the non-exclusive licence.
3. I confirm that granting the non-exclusive licence does not infringe other persons' intellectual property rights, the rights arising from the Personal Data Protection Act or rights arising from other legislation.

09.05.2022

1 The non-exclusive licence is not valid during the validity of access restriction indicated in the student's application for restriction on access to the graduation thesis that has been signed by the school's dean, except in case of the university's right to reproduce the thesis for preservation purposes only. If a graduation thesis is based on the joint creative activity of two or more persons and the co-author(s) has/have not granted, by the set deadline, the student defending his/her graduation thesis consent to reproduce and publish the graduation thesis in compliance with clauses 1.1 and 1.2 of the non-exclusive licence, the non-exclusive license shall not be valid for the period.